(NASA-CR-170467) MODELING THE THERMAL STRUCTURE AND MAGNETIC PROPERTIES OF THE CRUST OF ACTIVE REGIONS WITH APPLICATION TO THE RIO GRANDE RIFT Final Report (Business and Technological Systems, Inc.) 33 p G3/46

N83-16994

Unclas 08313

BTS

In 12-23-82

BTS33-82-88/rb
1018

BUSINESS AND TECHNOLOGICAL SYSTEMS, INC.
Aerospace Building, Suite 440
10210 Greenbelt Road
Seabrook, Maryland 20706

FINAL REPORT
MODELING THE THERMAL STRUCTURE AND MAGNETIC PROPERTIES OF THE CRUST OF ACTIVE REGIONS WITH APPLICATION TO THE RIO GRANDE RIFT

under
Contract NAS5-26616

NATIONAL AERONAUTICS AND SPACE ADMINISTRATION
Goddard Space Flight Center
Greenbelt, Maryland 20771

1.0 INTRODUCTION

This report summarizes the results of experiments in Curie depth estimation from long wavelength magnetic anomalies using methodologies previously developed in connection with satellite data, both Pogo-series (Mayhew et al, 1980; Mayhew, 1982a,b) and Magsat (Mayhew, 1982c). The heart of the work is equivalent-layer-type magnetization models derived by inversion of high-elevation, long wavelength magnetic anomaly data. The methodology is described in detail in the above references. The magnetization model for the United States used in Part 1 of the present work is given in Mayhew (1982c), and in Figure 1 of this report.

The central goal of the analysis is to find a magnetization distribution in a thin equivalent layer at the Earth's surface having maximum detail while retaining physical significance, and giving rise to a synthetic anomaly field which makes a best fit to the observed field in a least squares sense. Multiplying the magnetization distribution by the layer thickness gives the distribution of the vertical integral of magnetization in the magnetic crust to within an indeterminant ambiguity in level (Mayhew, 1982b). Such a model can be transformed to a more physically meaningful model given some independent constraints, as described below and in Mayhew (1982b). The apparent magnetization contrast (Δm) in the equivalent layer is approximated using an array of dipoles distributed in equal area at the Earth's surface. The dipoles are pointed in the direction of the main magnetic field, which carries the implicit assumption that crustal magnetization is dominantly induced or viscous. A key element of the analysis is the determination of the closest possible dipole spacing giving a "stable" inversion to a solution having physical significance. This is accomplished by plotting the standard deviation of the solution parameters (i.e. the magnetization values associated with the dipoles) against their spatial separation for a series of solutions. At separations closer than some critical one, the magnetization values become large (positive and negative) and no longer contour systematically. For Pogo data, the resolution limit is at about 300 km separation. This is to be compared with a similar result based on Magsat data which implies a resolution limit

approaching 200 km for this lower data. Mayhew (1982a) shows how to find a magnetization distribution on a grid twice as fine as that at the resolution limit, and this technique has been used in producing the Δm model shown in Figure 1.

One of the most straight forward approaches to interpretation is to attempt to convert the equivalent layer Δm models to models of thickness variation in a layer of constant magnetization. This is applicable, for example, to the case in which magnetic field variations reflect undulations of the Curie isotherm within the crust. The methodology is described in Mayhew (1982b). The vertical integral of magnetization implied by the Δm model is $H(M+\Delta m)$, where H is the equivalent layer thickness (arbitrarily taken to be 40 km), and M is the level ambiguity in the solution, assumed to be constant. For the case of thickness variation h in a layer of constant magnetization μ, the vertical integral of magnetization is $h\mu$. These two cases are indistinguishable in the anomaly field at satellite elevation, so equating the two gives a basic equation

$$H(M+\Delta m) = \mu h. \qquad (1)$$

For the Curie depth problem, if its depth can be estimated at at least two places (by use of thermal models or spectral estimates) the unknown M and μ can be estimated, and h determined for the whole region from the Δm distribution. The implied Curie depth configuration can then be used to constrain a regional crustal geothermal model. Results of this type are given in Section 2.

The resolution obtainable in such Curie depth models is limited by the data elevation. Mayhew (1982b) suggested that much higher resolution models could be obtained using upward continued aeromagnetic data in an analogous manner, where data coverage over a sufficiently large region is available. Part 2 of the present work is a test of this idea; results are described in Section 3.0.

To summarize the principal elements of the statement of work for this project, they are 1) to derive two-dimensional Curie depth models for several areas of the western U.S. using the equivalent-layer magnetization model derived from Magsat data, use the results to constrain finite-element thermal models, and compare theoretical heat flow predicted by the models with that inferred from direct measurements, and 2) to investigate the applicability of the Curie depth modeling methodology developed for satellite data to upward continued aircraft data.

2.0 PART 1: TWO-DIMENSIONAL THERMAL MODELS

The production of regional heat flow maps is problematical for a number of reasons. Heat flow data sets are inherently "noisy" because of various transient, ground water, topographic, and other effects. Measurements are irregularly distributed and of variable quality. Conductive heat flow is difficult to separate from convective effects due to local movements of hydrothermal fluids or magmas in active areas. Curie isotherm undulations should be reflected in regional heat flow variations. To the extent that Δm anomalies are due to Curie depth variations, they can be used along with heat flow measurements to guide the construction of regional heat flow maps. Such an approach was used by Mayhew (1982c) to make a regional heat flow map for the western U.S. (Figure 2), which was shown to compare favorably with similar maps made by others based principally on borehole measurements (Blackwell, 1979) and on silica geothermometry (Swanberg et al, in press). The first part of the present work was an investigation of whether Δm maps can be used in a more quantitative fashion to accurately predict heat flow and Curie depth.

2.1 Approach

Four section lines were chosen for two-dimensional analysis (Figure 1). These lines cross the boundaries of regional heat flow provinces inferred from measurements, characteristics of which are summarized briefly as follows. The whole of the Basin and Range is a heat flow high except for a low area in southern Nevada which may or may not reflect crustal heat conduction (Lachenbruch and Sass, 1977). The Basin and Range high extends around the southern margin of the Colorado Plateau (in a poorly-defined fashion) to the Rio Grande Rift, clearly a linear zone of high heat flow, although measured values scatter greatly. The Colorado Plateau has lower heat flow than surrounding regions, although generally higher than "normal". The axis of the Sierra Nevada has low heat flow. These gross characteristics show up in regional heat flow maps, and are reflected in the Δm map (Figure 1). Low Δm values apparently reflect shallow Curie depths on a regional scale, and thus high conductive crustal heat flow.

Δm variations along the four section lines were transformed to Curie isotherm configuration in the following manner. The basic equation is (1), from which variations in magnetic crustal thickness h are computed from variations in Δm. Estimates are needed for the parameters M and μ in equation (1). These are gotten by fitting a line to a plot of estimates of range of h derived from spectral depth estimates, depth to 550°C (the assumed Curie temperature) given by thermal models constrained by surface heat flow measurements, or, in the case of the Sierra Nevada, seismic estimates of depth to mantle, against range of Δm for the corresponding areas. The Moho is assumed to be the magnetic bottom for the Sierras, since the very low heat flow values measured along the axis of the belt imply depths to 550° well into the mantle, which is assumed to be non-magnetic (Wasilewski et al, 1979). The plot is given as Figure 3. The ranges of values are rather large, but give an overall trend in the right direction. Two lines are run through the data. One is an eyeball best fit, and implies M and μ of 0.72 and 1.11 A/m, respectively. The other implies $M = 0.95$, $\mu = 2.00$ A/m, and was used mainly to give a comparison, although the values are similar to those inferred from a preliminary study of the southern Rio Grande Rift (Mayhew, 1982b). Both pairs of parameters were used in the modeling.

The Curie surface configurations (assumed to be isothermal and equal to 550° on all sections but one) were used to constrain a finite-element thermal model. This software was further developed from that used previously (Mayhew, 1982b). Numerous runs were made. Most involved a simple one-layer model with surface heat production decreasing decrementally with depth from a surface value A_0, and constant thermal conductivity K. Values for A_0 and K of 5 HPU and 6 (cgs), respectively, were used as starter values, and are those suggested by Diment et al (1975) as typical for the crust, although measured values on crystalline rocks have a great range. Other values were tried as well, as were two-layer models. It was found that the overall results are not profoundly affected by the choice of reasonable thermal parameters.

2.2 Results

Figure 4 (Section 1) is a section extending from the Pacific coast to the Great Plains. Δm is the apparent magnetization contrast along the section from Figure 1. Also shown are the Curie depth surfaces (hc) for the two pairs of (M,μ) mentioned above and the computed heat flow profile associated with each thermal model. The circles represent heat flow measurements within about 100 km of the section. While they are characteristically scattered, they are in good general agreement with predicted heat flow, especially model A. The results seem to confirm the existence of zones of elevated heat flow in the Basin and Range adjacent to the Wasatch Front and along the northern extension of the Rio Grande Rift.

Figure 5 (Section 2) crosses from the southern Basin and Range to the Colorado Plateau. Both models predict about the same high heat flow (3 HFU) south of the Colorado Plateau. Model 2B predicts a heat flow level quite similar to that associated with the Plateau (about 1.5 HFU). The Curie surfaces are quite different; that for model A is at Moho depth beneath the Plateau, but well up into the crust for model B.

Section 3 (Figure 6) crosses the central Rio Grande Rift. Model A was computed assuming one layer with A_0 and K equal to 5.0 and 6.0, respectively. For comparison, a two-layer model assuming $K = 6.5$ in an upper layer 20 km thick and a lower layer with $K = 5.0$, and with heat production A_0 equal to 5.3 in the upper layer and constant in the lower layer and equal to the decremental value at 20 km, (i.e. $A_2 = A_0 \exp(-20/D)$, was computed. D, the decremental constant, is taken to be 10 km, the value generally assumed for the western U.S. The other parameters are like those favored by Blackwell (1971). The computed heat flow profile is very close to model A. Model B also assumed one layer with $A_0 = 5.0$ and $K = 6.0$, but different (M,μ). The Curie surface for this model is shown. Wasilewski (personal communication) has measured low Curie points on lower crustal xenoliths from the southern Rio Grande Rift (about 300°C) and has speculated that this is a general characteristic of the rift zone, and the effect of reducing conduction in a hot, dry environment at deep crustal

levels. More "normal" values (around 550°C) are measured for the Colorado Plateau. Model C is for a hypothetical case in which the Curie surface is not isothermal, but varies from 550° on the flanks of the rift to 300° within the rift, with abrupt 50 km transitions between. The transitions are centered on about 400 and 600 km along the section line. The model gives lowered heat flow within the rift, as anticipated, which is clearly in disagreement with measurements. This is only an interesting exercise, however, because at present very little information is available on the extent of the low Curie points (laterally and vertically) and the location and widths of the transition zone to constrain such a model.

Also shown in Figure 6 are measured heat flow values within 100 km of the section line and the heat flow profile given by Figure 2, which is based on averages. The measurements scatter so badly that it is difficult to judge the models, although predicted heat flow of model A is probably too low, both for the rift and the Colorado Plateau.

Figure 7 is from the southern Rio Grande Rift (Section 4), where measured heat flow tends to be higher on the average than further north. This is reflected in the Δm distribution and in the resulting thermal models.

3.0 PART 2: INVERSION OF CONTINUED AEROMAGNETIC DATA

This part of the project was an investigation of whether aeromagnetic data could be used to infer a Curie surface by a method analogous to that used with satellite data on a larger scale. The data set for this study was from the central Oregon Cascades flown by Oregon State University. It was chosen because 1) the data is readily available on tape from the NOAA data center in a form suitable for easy grid averaging, 2) it is in a geothermally active region, 3) it is of sufficient extent for valid analysis, and 4) a Curie depth study has already been carried out on this data set by Connard (1979). Connard carried out depth-to-magnetic-bottom computations by operations in the two-dimensional frequency domain, using methodology made popular by a number of previous investigators, notably Spector and Grant (1970). Certain authors have applied the frequency-domain approach to finding the configuration of the bottom of a magnetized layer, for example Gerard and Debeglia (1975) and Hahn et al (1976). It seemed that Connard's results would provide an interesting comparison with those of the present study.

3.1 Approach

The data was gridded, with grid spacing equal to the flight line spacing (1 mile = 1.61 km). A 76(x) by 80(y) matrix resulted. It was found that not all the data was present on the tape, and a block of values had to be filled in by hand, using Connard's original map (Figure 8). With this labor and elimination of some bad values a nice contour map was produced (Figure 9) which compares favorably with Connard's. This data was to be upward continued, and to reduce edge effects the grid area was extended by simply folding the data over in a 25 km strip around the border (Figure 10).

Our hypothesis is that at altitudes which are "large" with respect to the thickness of the magnetic crust, discrete "local" sources will be minimal, that the data will predominantly reflect variations in magnetic crustal thickness, and that to a good approximation the magnetization of the

layer will appear to be uniform. We imagine a Curie surface level undulating about some intermediate level which we take as the bottom of an equivalent layer. We determine a magnetization variation in the equivalent layer by inversion, then transform this to thickness variations in a layer of constant magnetization under the assumption that the fields due to two such models are virtually indistinguishable in the data.

Rather than approximating the source model with dipoles, the equivalent layer was subdivided into several arrays of vertical rectangular prisms, with block widths determined by the number specified in each direction. Several inversions were then made for the several arrays to determine the resolution achievable, by plotting the standard deviation of the magnetization values in the solutions against the block spacing (or number of blocks in each dimension).

Connard's results suggest shallow Curie depths of around 6-14 km. We therefore selected an equivalent layer thickness of 10 km. The data was upward continued to 25 km (Figure 11) which experience suggests is a more than sufficiently "large" altitude. The continued data was then inverted to a series of solutions.

3.2 Results

The results of the inversions are given in Table 2. A plot of parameter standard deviation against number of blocks in each direction is shown in Figure 12. It suggests that the unstable region is entered at block spacing of about 25 km (5 x 5 array of blocks).

To convert block magnetization values in the equivalent layer to thickness (Curie depths), we reason as follows. The vertical integral of magnetization in a block (i) of variable thickness h_i and constant magnetization μ is μh_i. The vertical integral of magnetization in the equivalent layer of thickness H we take to be $H(\mu + \Delta m_i)$, where the Δm are the magnetization values solved for. We equate the two, and if H and μ can be estimated, the h_i can be found. The results obviously

depend on some independent estimate of overall Curie depth level, either from spectral estimates or from some thermal model. For μ we can go two ways. We can assume a value and see if reasonable Curie depths result. We took a second approach. Connard's results indicate a range of depths of 6 to 14 km. We assumed that the minimum Δm in the solution was associated with a 6 km Curie depth, the maximum with the 14 km level, and thus were able to solve for μ; then we could ask whether it was a reasonable value. For the 5 x 5 array μ is about 1 A/m, a reasonable value. For, say, the 8 x 8 array $\mu = 6$ A/m, a value commonly associated with mafic plutons or flows, but perhaps high for crustal rocks generally.

The depths computed for a 5 x 5 array are shown in Figure 13. Clearly, they are in agreement with the continued field variations. Figure 14 shows the depths for the 3 x 3 solution for comparison with Connard's results, since he subdivided the area into 3 x 3 blocks and carried out spectral analysis on each separately, although only four of the nine spectra showed the spectral peak required for a depth estimate. His results are reproduced in Figure 15. The comparison is only fair. In particular, the continuation of the central zone of shallow depths to the north suggested by Figure 15 is not supported by Figure 14. On the other hand, both maps predict relatively deep magnetic bottom on the left (west) side. Both methodologies are based on simplifying assumptions and considerable treatment of the data; further comparisons of them will be possible when heat flow data from the survey area is available.

REFERENCES

Ander, M. E., Geophysical study of the crust and upper mantle beneath the central Rio Grande Rift and adjacent Great Plains and Colorado Plateau. Los Alamos Scientific Laboratory Report LA-8676-T, 218 pp., 1981.

Bhattacharyya, B. K., and L. K. Leu, Analysis of magnetic anomalies over Yellowstone National Park: Mapping of Curie point isothermal surface for geothermal reconnaissance, J. Geophys. Res., 80, 4461-4465, 1975.

Blackwell, D. D., The thermal structure of the continental crust, in The Structure and Physcial Properties of the Earth's Crust, Geophys. Monogr. Ser., vol. 14, edited by J. D. Heacock, pp. 169-184, AGU, Washington, DC, 1971.

Blackwell, D. D., Heat flow and energy loss in the western United States, Mem. Geol. Soc. Am. 152, 175-208, 1979.

Connard, G. G., Analysis of aeromagnetic measurements from the central Oregon Cascades. M. S. Thesis, Oregon State University, 1979.

Cordell, L., Regional gephysical setting of the Rio Grande Rift, Geol. Soc. Am. Bull., 89, 1073-1090, 1978.

Diment, W. H., T. C. Urban, J. H. Sass, B. V. Marshall, R. J. Munroe, and A. H. Lachenbruch, Temperatures and heat contents based on conductive transport of heat, U. S. Geological Survey Circ. 726, 84-103, 1975.

Eaton, G. P., R. R. Wahl, H. J. Prostka, D. R. Mabey, and M. D. Kleinkopf, Regional gravity and tectonic patterns: Their relation to late Cenozoic epeirogeny and lateral spreading in the western cordillera, Mem. Geol. Soc. Am. 152, 51-91, 1979.

Galliher, S. C. and M. A. Mayhew, On the Possibility of detecting large-scale crustal remanent magnetization with Magsat vector magnetic anomaly data. Geophysical Research Letters 9, 325-328, 1982.

Gish, D. M., G. R. Keller, and M. L. Spar, A refraction study of deep crustal structure in the Basin and Range - Colorado Plateau of eastern Arizona, J. Geophys. Res. 86, 6029-6038, 1981.

Hahn, A., E. G. Kind and D. C. Mishra, Depth estimation of magnetic sources by means of Fourier amplitude spectra. Geophysical Prospecting 24, 287-308, 1975.

Keller, G. R., L. W. Braile, and P. Morgan, Crustal structure, geophysical models and contemporary tectonism of the Colorado Plateau, Tectonophysics 16, 131-147, 1979.

Lachenbruch, A. H., and J. H. Sass, Heat flow in the United States and the thermal regime of the crust, in The Nature and Physial Properties of the Earth's Crust, Geophys. Monogr. Ser., Vol. 20, edited by J. G. Heacock, 625-675, AGU, Washington, D.C., 1977.

Mayhew, M. A., Initial equivalent layer magnetization model for the United States based on Magsat data. EOS 62, 270, 1981.

Mayhew, M. A., An equivalent layer magnetization model for the United States derived from satellite-altitude magnetic anomalies, Journal of Geophysical Research 87, 4837-4845, 1982a.

Mayhew, M. A., Application of satellite magnetic anomaly data to Curie isotherm mapping, Journal of Geophysical Research 87, 4846-4854, 1982b.

Mayhew, M. A., Magsat anomaly field inversion and interpretation for the U.S. Final Report, NASA Contract NAS5-26328, 1982c.

Mayhew, M. A., B. D. Johnson and R. A. Langel, An equivalent source model of the satellite-altitude magnetic anomaly field over Australia. Earth and Planetary Science Letters 51, 189-198, 1980.

Mayhew, M. A. and R. H. Estes, Simulations and software development related to Magsat data. Final Report, National Aeronautics and Space Administration/Goddard Space Flight Center Contract NAS 5-25720, Volume 1, 87 pp., 1980.

Mayhew, M. A. and R. H. Estes, Constrained inversion of satellite magnetic anomaly data. Final Report, National Aeronautics and Space Administration/Goddard Space Flight Center Contract NAS 5-25698, Volume 3, 68 pp., 1981.

McGetchin, R. R., and L. T. Silver, A crust-upper mantle model for the Colorado Plateau based on observations of crystalline rock fragments in the Moses rock dike, J. Geophys. Res., 77, 7022-7037, 1972.

Pakiser, L. C. and J. N. Brune, Seismic models of the root of the Sierra Nevada, Science 210, 1088-1094.

Roy, R. F., D. D. Blackwell, and E. R. Decker, Continental heat flow, in The Nature of the Solid Earth, edited by E. C. Robertson, pp. 506-543, McGraw-Hill, New York, 1972.

Sinno, Y. A., G. R. Keller and M. L. Spar, A crustal seismic refraction study in west-central Arizona. J. Geoph. Res. 86, 5023-5038, 1981.

Shuey, R. T., D. K. Schellinger, E. H. Johnson and L. B. Alley, Aeromagnetics and the transition between the Colorado Plateau and the Basin Range province, Geology, 1, 107-110, 1973.

Shuey, R. T., D. K. Schellinger, A. C. Tripp, and L. G. Alley, Curie depth determination from aeromagnetic spectra, Geophys. J. R. Astron. Soc. 50, 75-101, 1977.

Spector, A. and F. S. Grant, Statistical models for interpreting aeromagnetic data. Geophysics 35, 293-302, 1970.

Swanberg, C. A., and P. Morgan, Heat flow map the United States based on silica geothermometry, in Physical Properties of Rocks, vol. II-2 edited by Touloukian, H. S., W. R. Judd, and R. F. Roy, in press, McGraw-Hill, 1982.

Thompson, G. A. and M. L. Zoback, Regional geophysics of the Colorado Plateau. Tectonophysics 35, 293-302, 1970.

Wasilewski, P. J. and E. Padovani, Magnetization in the lower crust (abstract), EOS Trans. AGU 61, 222, 1980.

Wasilewski, P. J., H. H. Thomas, and M. A. Mayhew, The Moho as a magnetic boundary, Geophys. Res. Lett., 6, 541-544, 1979.

TABLE 1

Parameters used in Curie depth/thermal
models of Figures 4-7

LINE	MODEL	M	MU	A_0	K
1	A	7.2	11.1	5.0	6.0
1	B	9.5	20.0	5.0	6.0
2	A	7.2	11.1	5.0	6.0
2	B	9.5	20.0	5.0	6.0
3	A	7.2	11.1	5.0	6.0
3	B	9.5	20.0	5.0	6.0
3	C	9.5	20.0	5.0	6.0
4	A	7.2	11.1	5.0	6.0
4	B	9.5	20.0	5.0	6.0

TABLE 2

NMBR	X	Y	SDF	PSD	MAX	MIN	MU
3	40	42	14.2	36	-3	-30	33
4	30	32	12.6	54	22	-34	70
5	24	25	11.6	67	56	-38	118
6	20	21	10.8	94	128	-95	278
7	17	18	10.3	120	178	-156	214
8	15	16	9.7	204	260	-214	591
10	12	13	8.8	651	439	-474	1142
12	10	11	8.0	28?5	1197	-1364	3201

NMBR = number of blocks in each direction

X, Y = block widths

SDF = standard deviation of fit of continued and computed fields

PSD = magnetization parameter standard deviation

MAX = maximum magnetization value in solution

MIN = minimum value

MU = computed magnetization

FIGURE CAPTIONS

Figure 1. Apparent magnetization contrast in 40 km thick layer derived by inversion of Magsat anomaly data. Contour interval 0.2 A/m. From Mayhew (1982c). Four section lines of Figures 4-7 shown. BR is Basin and Range, SR is Snake River Plain, CP is Colorado Plateau, R is Rio Grande Rift, S is Sierra Nevada, Wb and Db are Williston and Denver Basins, P is western boundary of Great Plains.

Figure 2. Contours of heat flow averaged over two staggered 200 km grids and guided by Δm distribution of Figure 1. Contour interval 0.5 hfu. From Mayhew (1982c).

Figure 3. Estimates of magnetic crustal thickness based on aeromagnetic spectra, depth to 550°C (assumed Curie temperature) from thermal models, or, for Sierran region, seismic crustal thickness. 1 is Sierras along 38°N, 2 is Sierras as a whole, 3 is Uinta Basin, 4 is Utah High Plateaus, 5 is Yellowstone, 6 is Colorado Plateau, 7 is southwestern Great Plains, 8 is Basin and Range as a whole, 9 is Rio Grande Rift. Data from Roy et al (1972), Pakiser and Brune (1980), Eaton (1963), Lachenbruch and Sass (1977), Shuey et al (1977), Cordell (1978), Bhattacharyya and Leu (1975), McGetchin and Silver (1972), Keller et al (1979), Stewart and Pakiser (1962), Blackwell (1971), Cook et al (1978,79), Decker and Smithson (1975), and Olsen et al (1979).

Figure 4. Section 1. Crustal seismic results from Eaton (1963), Cordell (1978), Jackson and Pakiser (1965), and Jackson et al (1963). Numbers are uppermost mantle velocities. M is Moho. Circles are heat flow values within about 100 km of the section (Grim et al, 1977). Heavy lines within crustal section labeled A,B are 550°C isotherms inferred from Δm curve as described in text. Light lines above labeled A,B are associated surface heat flow profiles computed from thermal model.

Figure 5. Section 2. Crustal seismic results from Warren (1969) and Roller (1965). Numbers and symbols as in Figure 4.

Figure 6. Section 3. Crustal seismic results from Gish et al (1981), Sinno et al (1981), Olsen et al (1979), and Stewart and Pakiser (1962). Other numbers and symbols as in Figure 4.

Figure 7. Section 4. Numbers and symbols as in Figure 4.

Figure 8. Cascades aeromagnetic survey (from Connard, 1979).

Figure 9. Contour map of digitized Cascades data set used in present study. Units: Hundreds of nT, contour interval 200nT.

Figure 10. As Figure 9, with border of extended data.

Figure 11. Data of Figure 10 upward continued to 25 km. Units: nT, contour interval 5nT.

Figure 12. Magnetization parameter standard deviation plotted against block width. Numbers beside dots indicate number of blocks in each direction within survey area.

Figure 13. Computed depths to magnetic bottom superimposed on Figure 11 data for original map area. 5 x 5 solution.

Figure 14. As Figure 13 for 3 x 3 solution.

Figure 15. Magnetic depth results and interpretation of Connard (1979).

ORIGINAL PAGE IS
OF POOR QUALITY

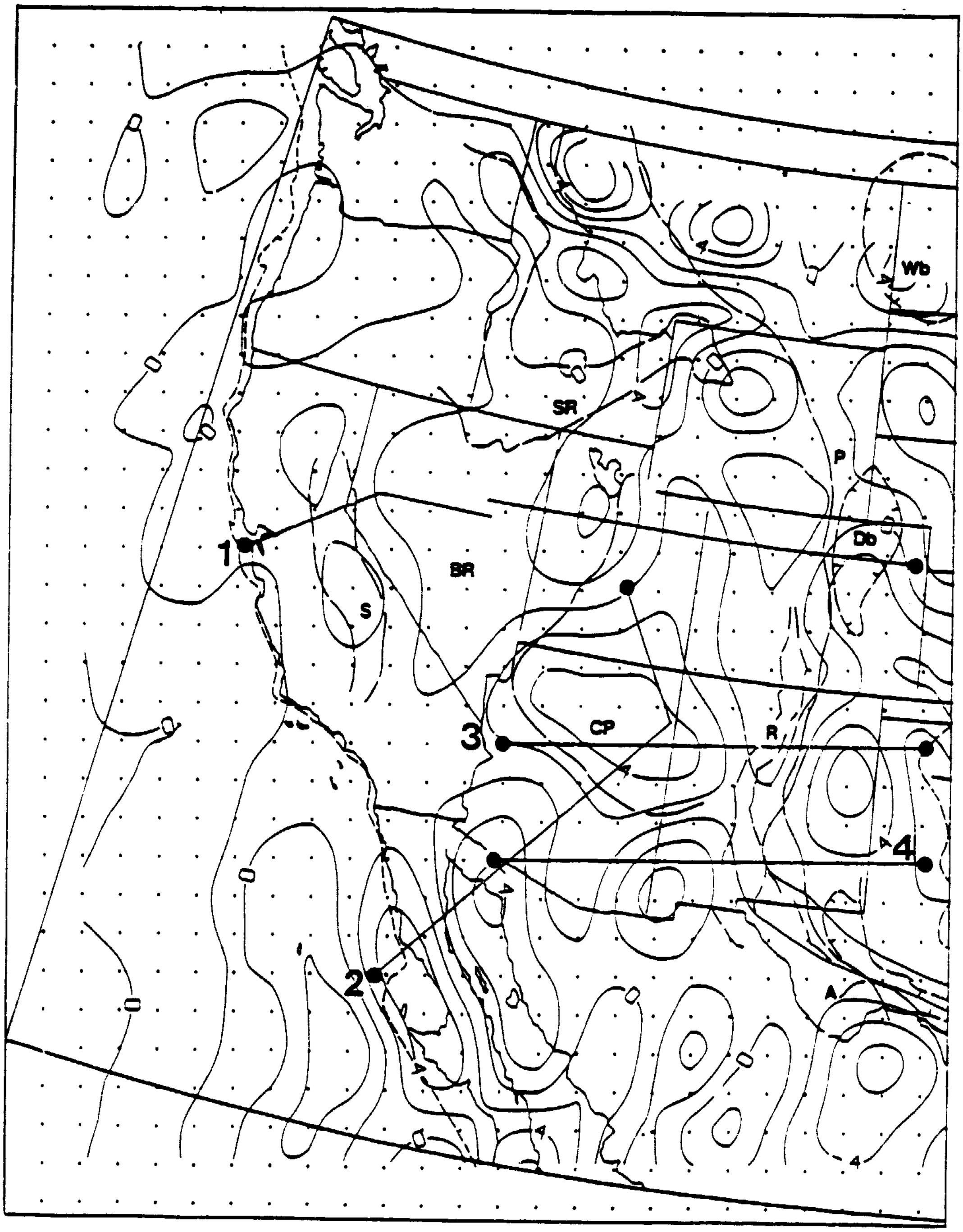

Figure 1

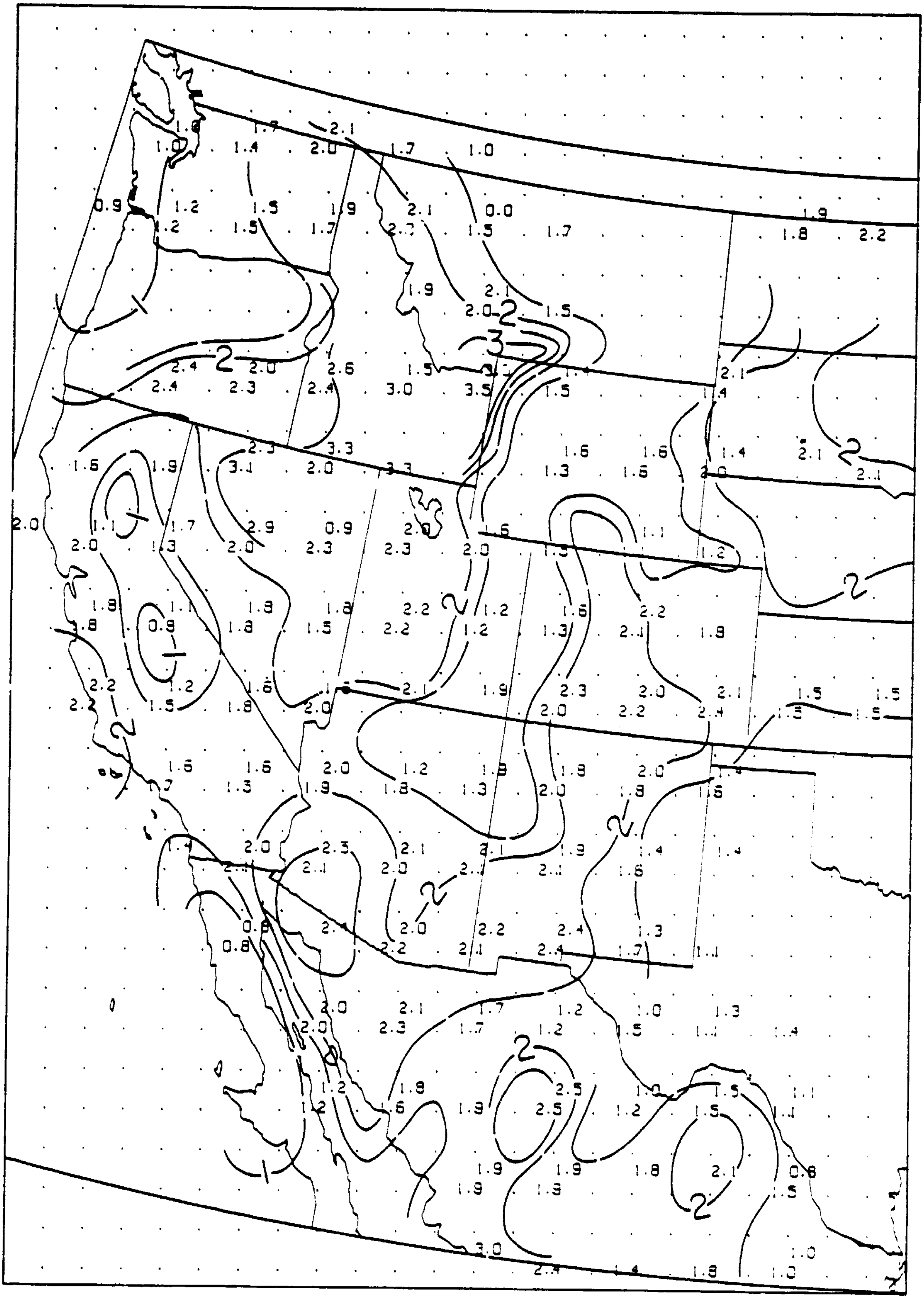

Figure 2

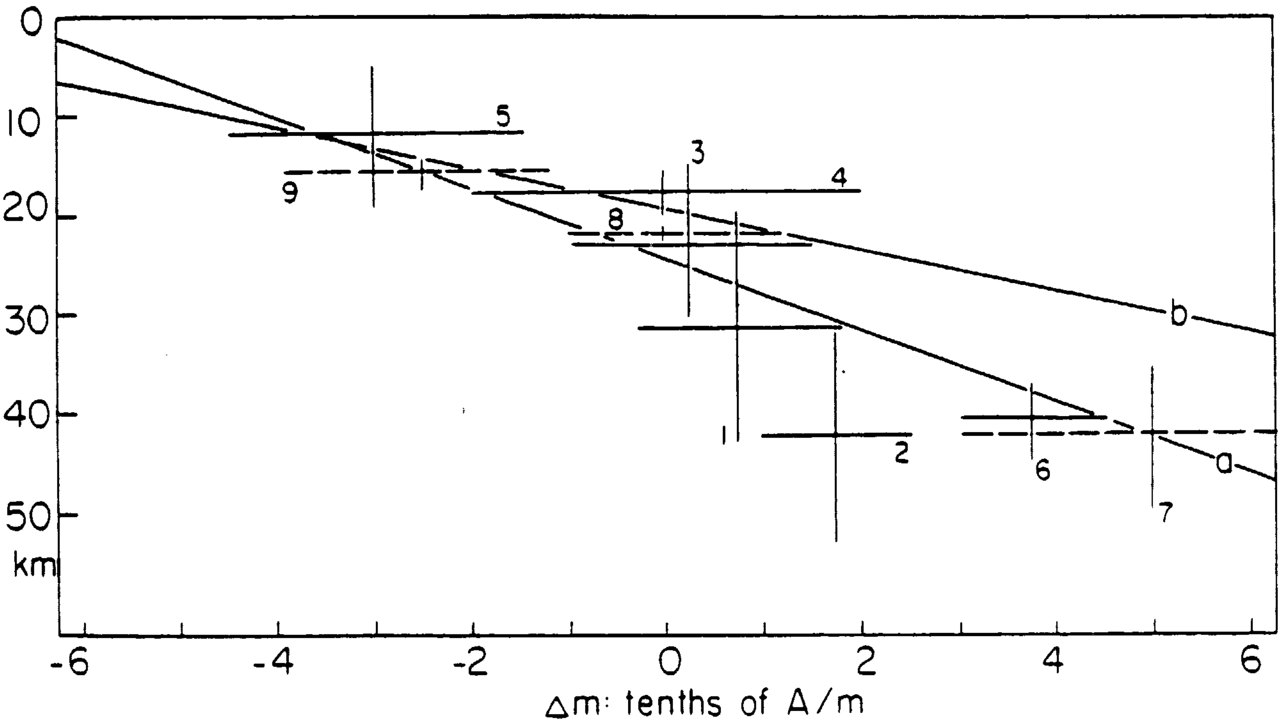

Figure 3

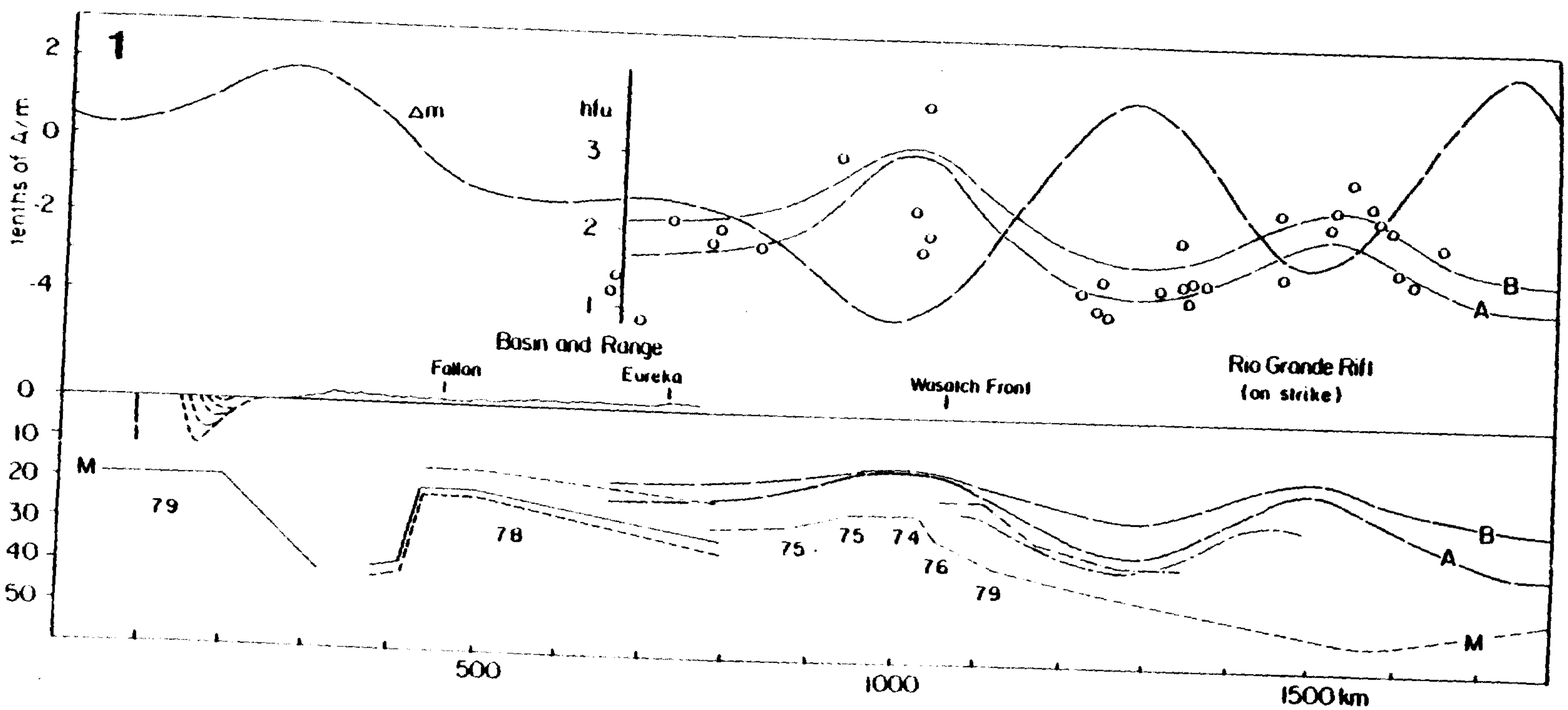
1
tenths of Δ/m
Δm
hfu
Basin and Range
Fallon
Eureka
Wasatch Front
Rio Grande Rift
(on strike)
B
A
M
79
78
75
75
74
76
79
500
1000
1500 km

Figure 4

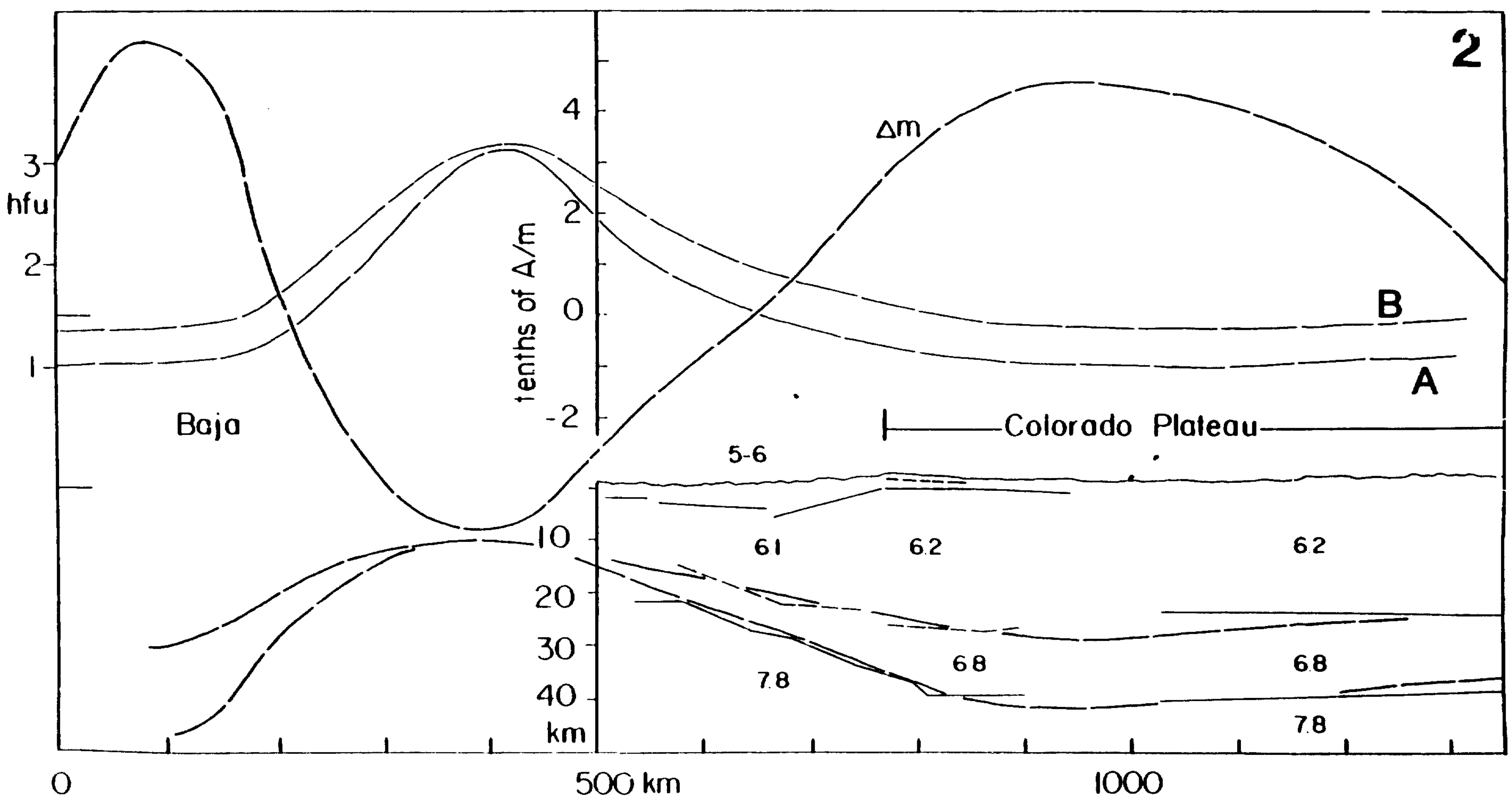
2
3
hfu
2
1
Baja
4
2
0
-2
tenths of A/m
Δm
B
A
Colorado Plateau
5-6
6.1
6.2
6.2
10
20
30
40
km
7.8
6.8
6.8
7.8
0
500 km
1000

Figure 5

ORIGINAL PAGE IS
OF POOR QUALITY

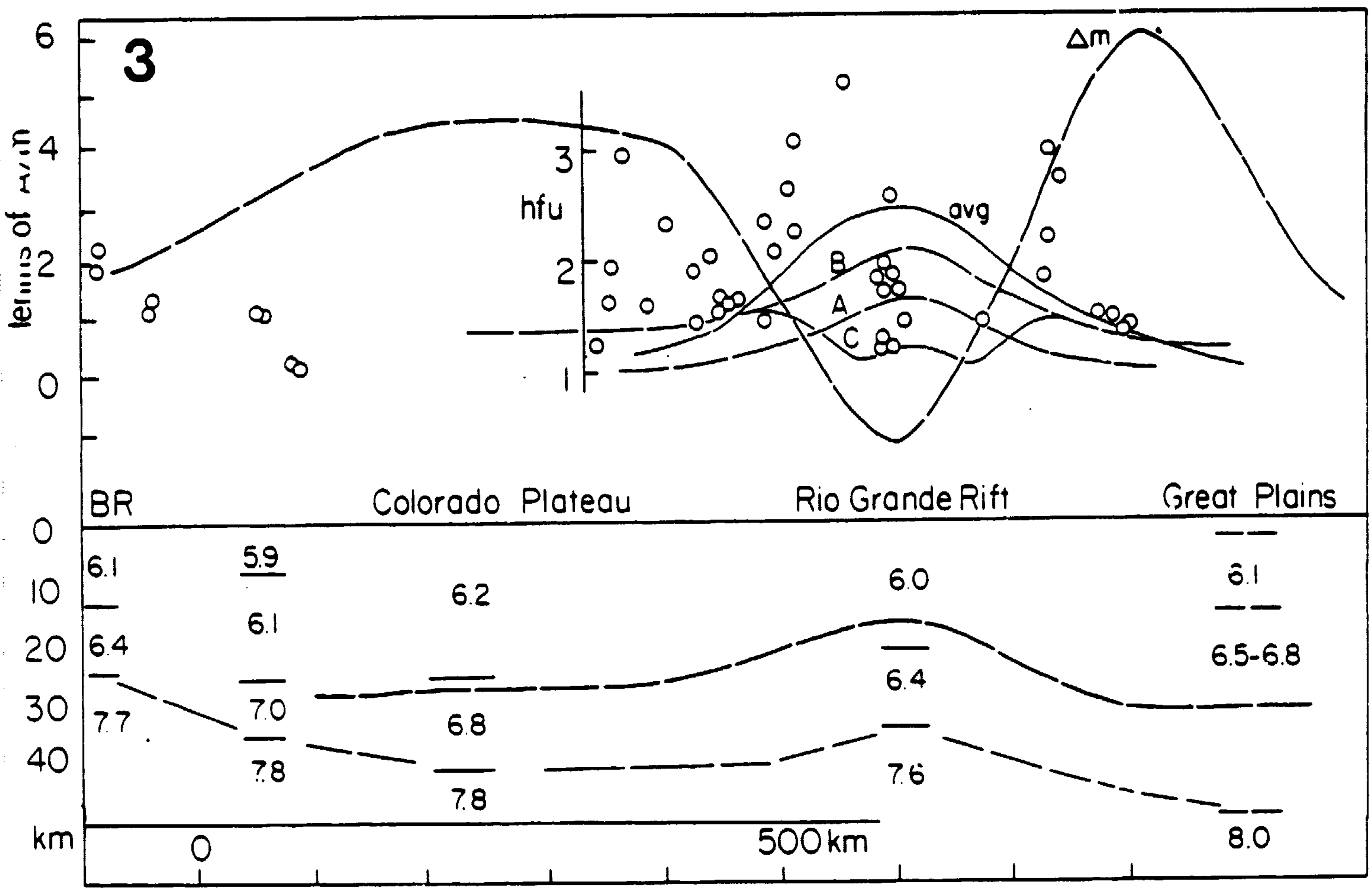

Figure 6

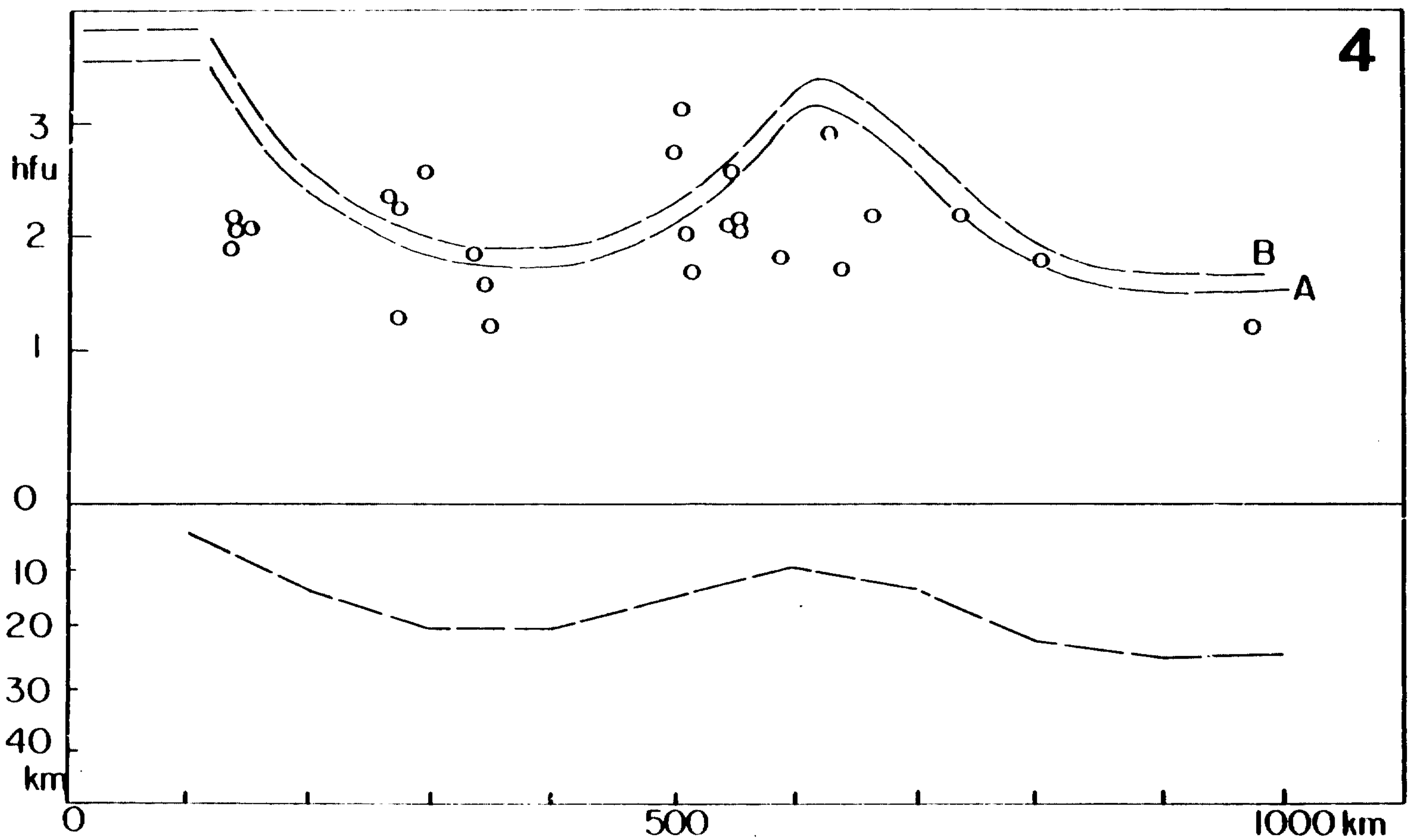

Figure 7

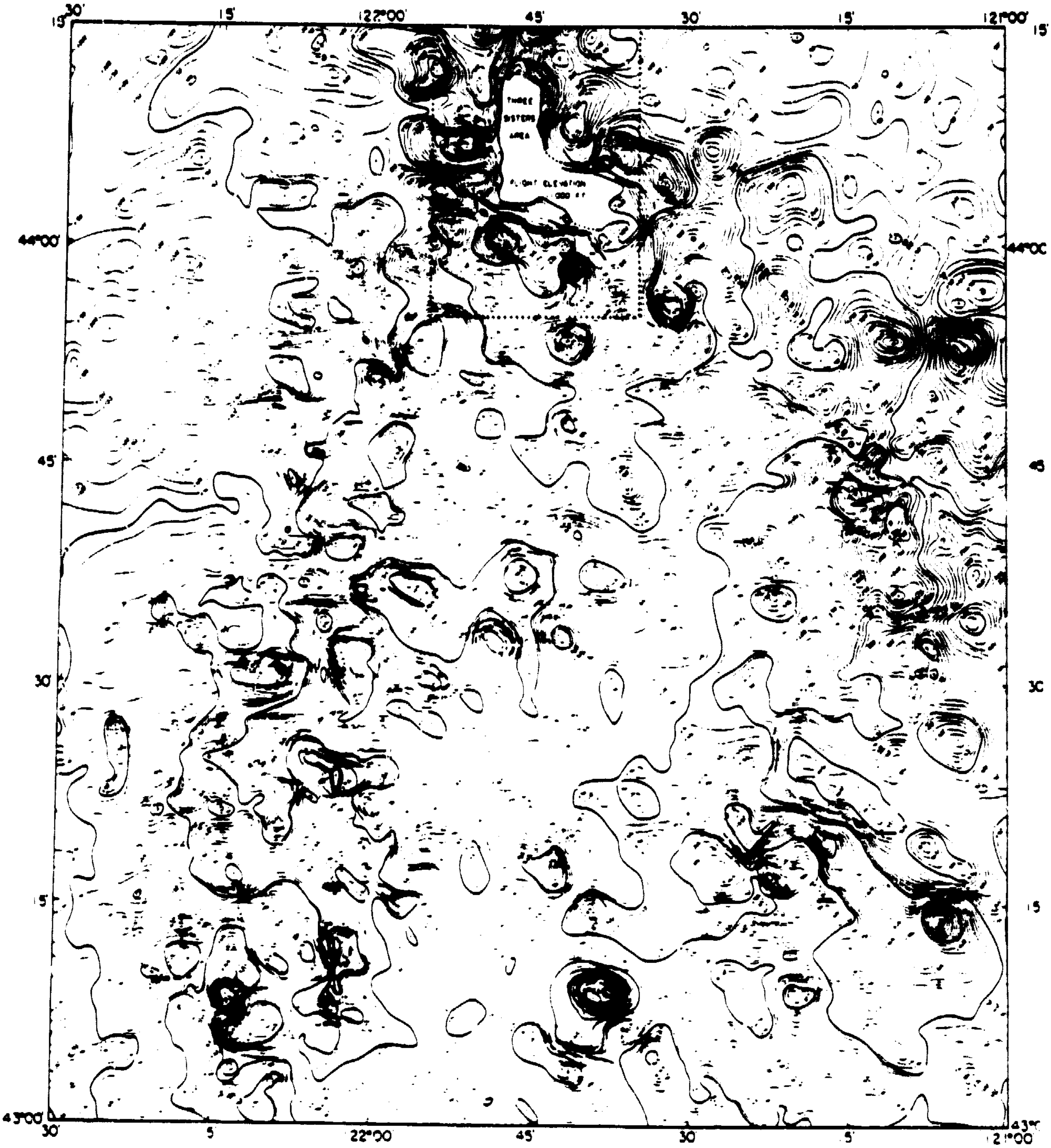

TOTAL FIELD AEROMAGNETIC ANOMALY MAP
CASCADE MOUNTAIN RANGE, CENTRAL OREGON

TOTAL FIELD DATA FROM
GEOPHYSICS GROUP OSU 1977
FLIGHT ELEVATION 9,000 FT

KILOMETERS

MILES

UNIVERSAL TRANSVERSE MERCATOR PROJECTION
CONTOUR INTERVAL 50 GAMMAS
SCALE 500,000

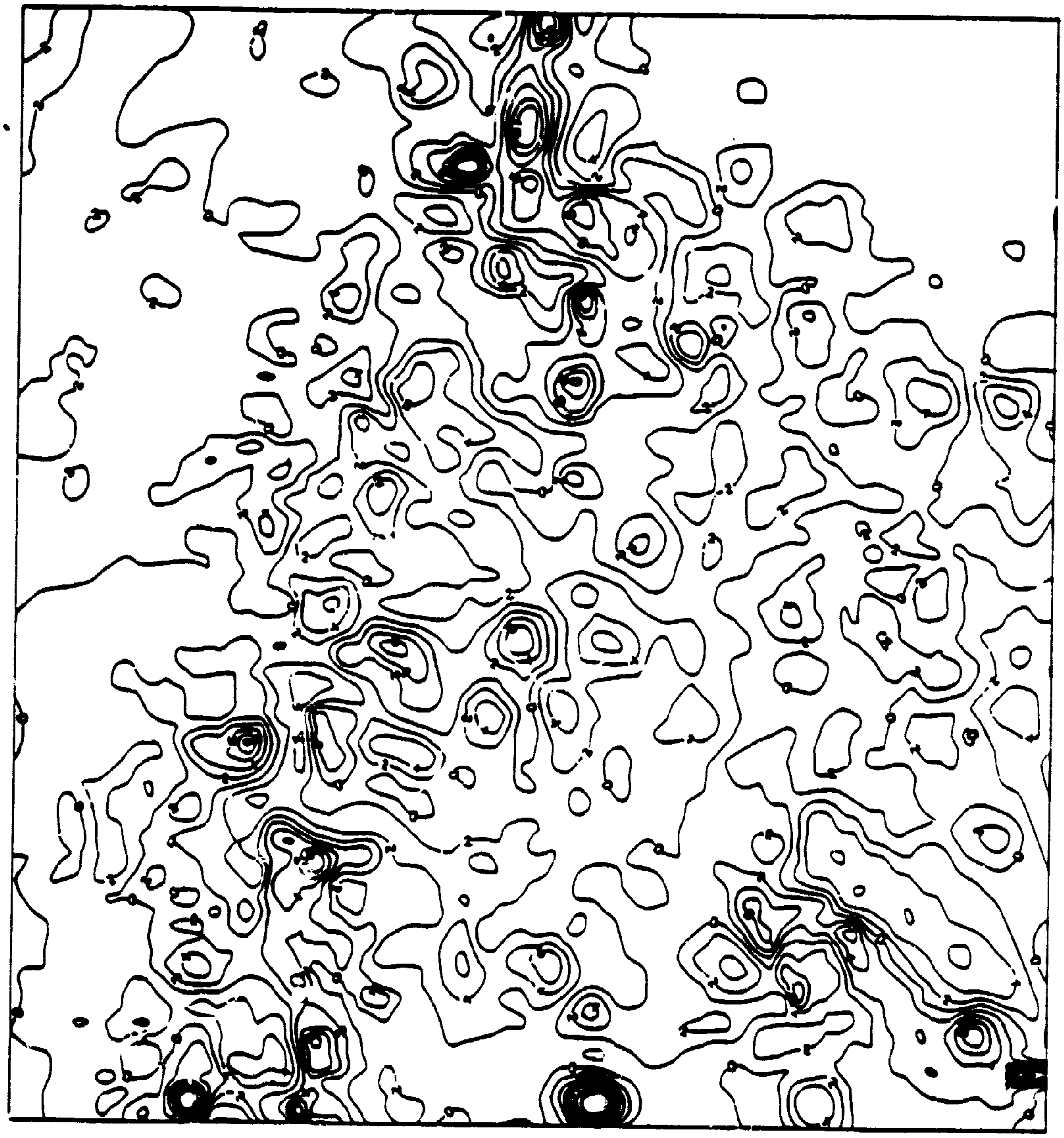

Figure 9

ORIGINAL PAGE IS
OF POOR QUALITY

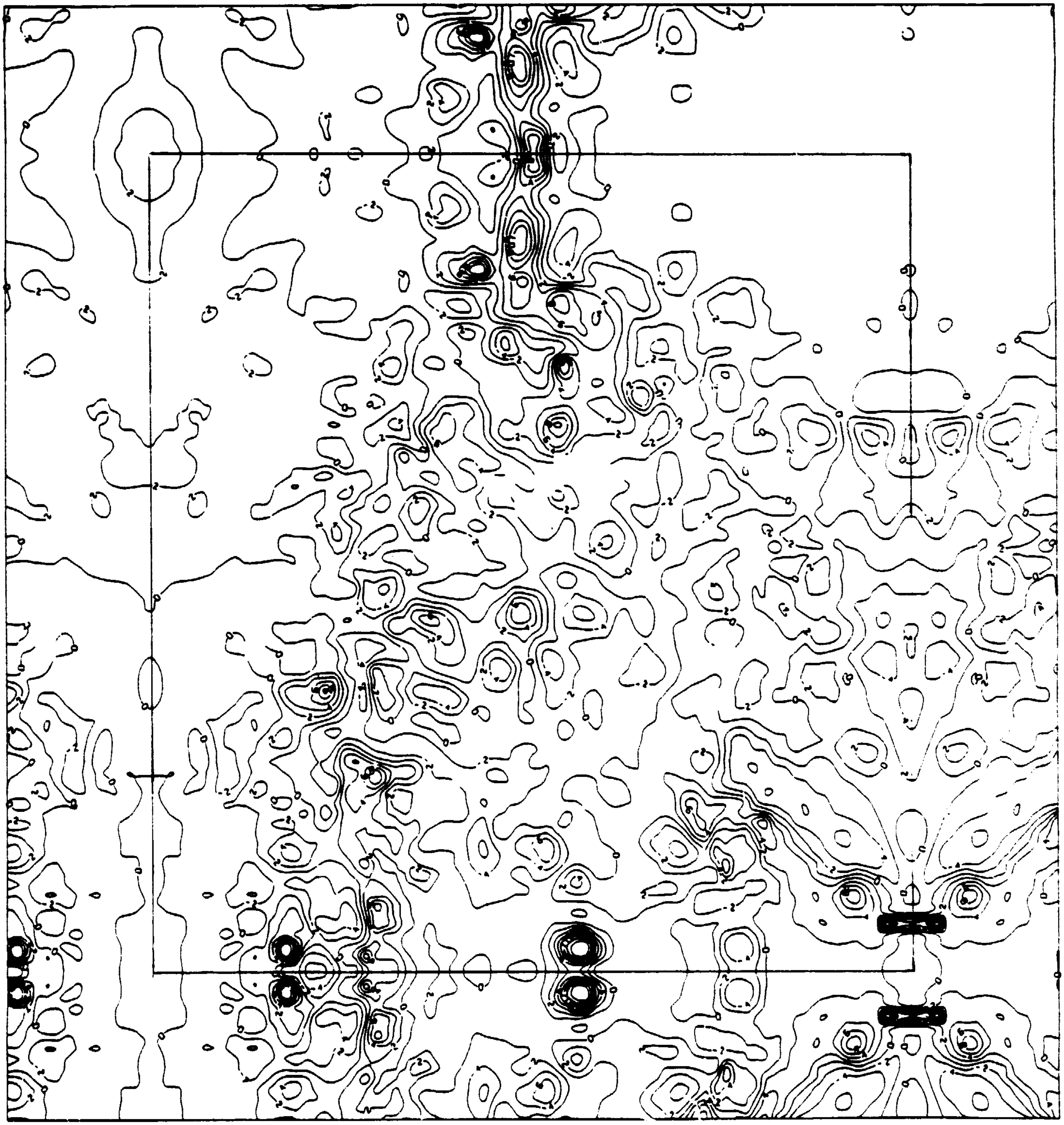

Figure 10

ORIGINAL PAGE IS
OF POOR QUALITY

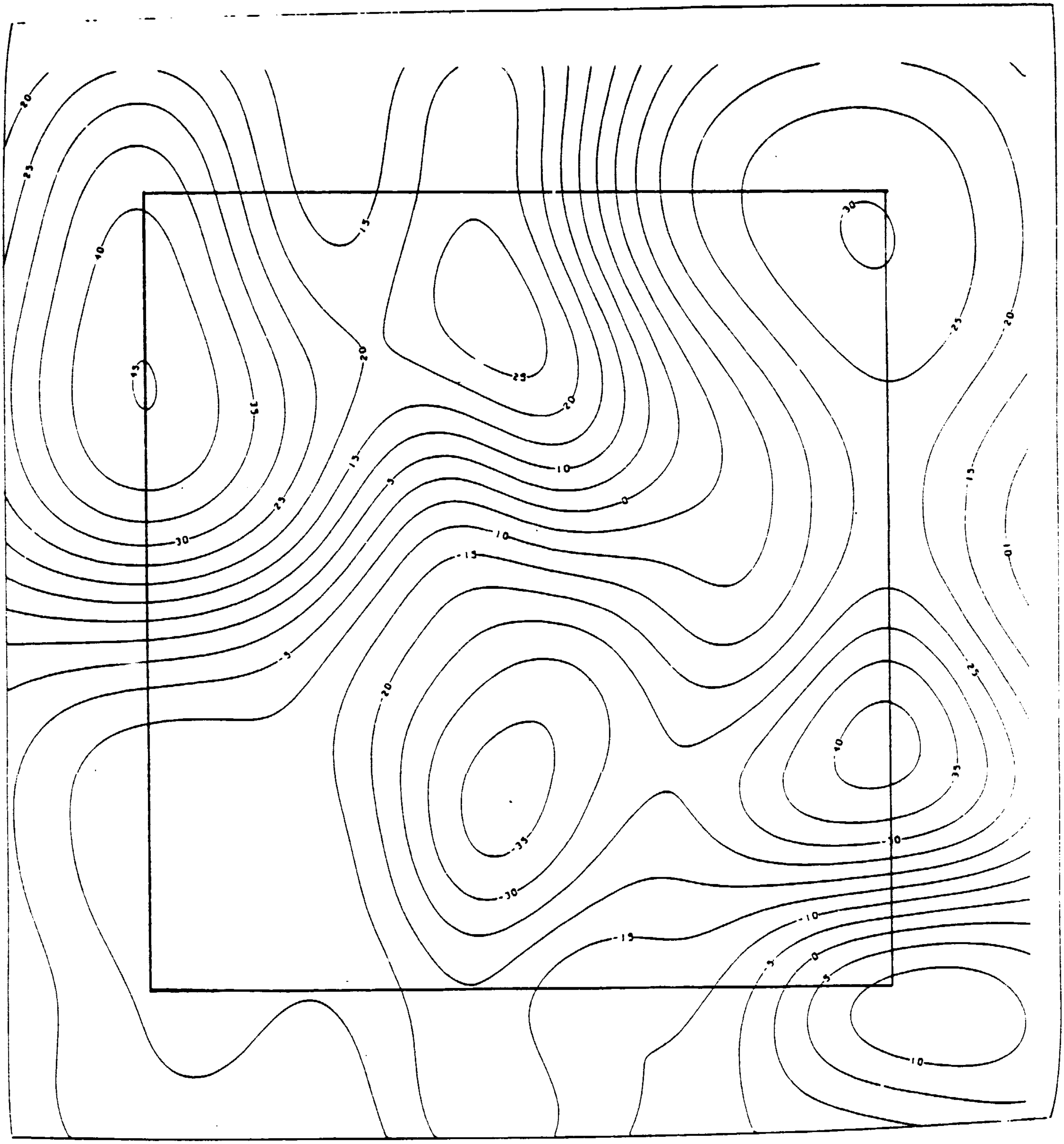

Figure 11

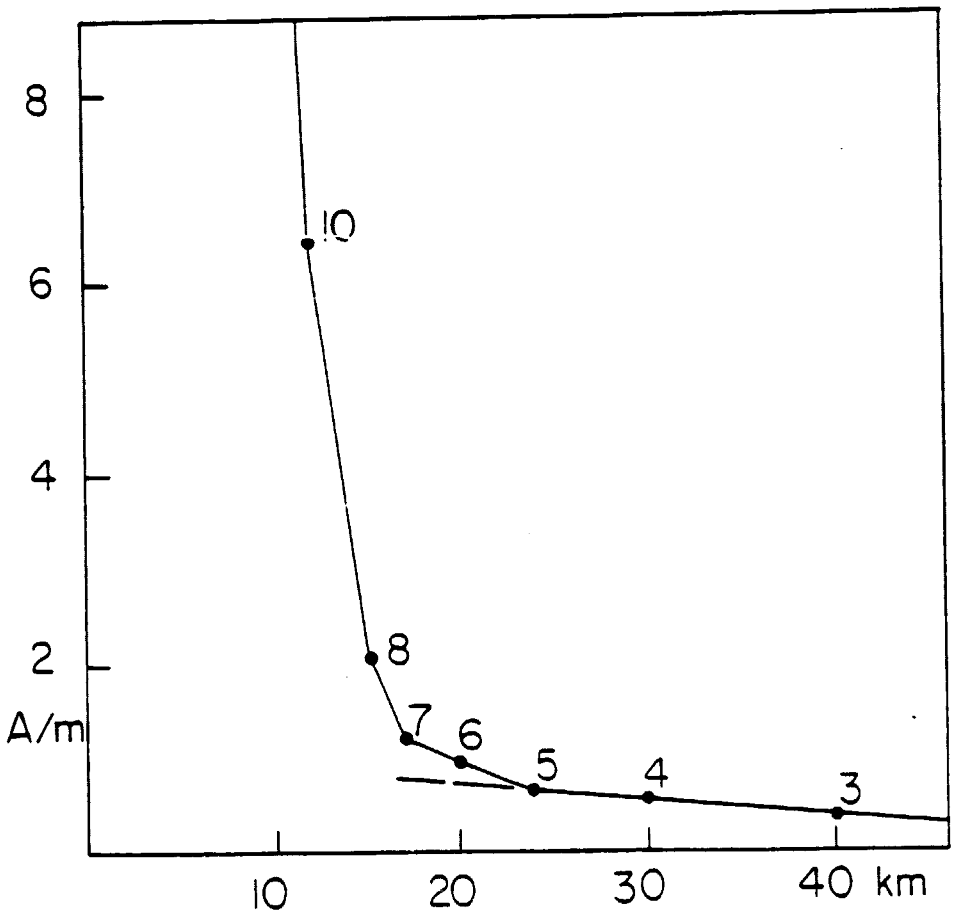

Figure 12

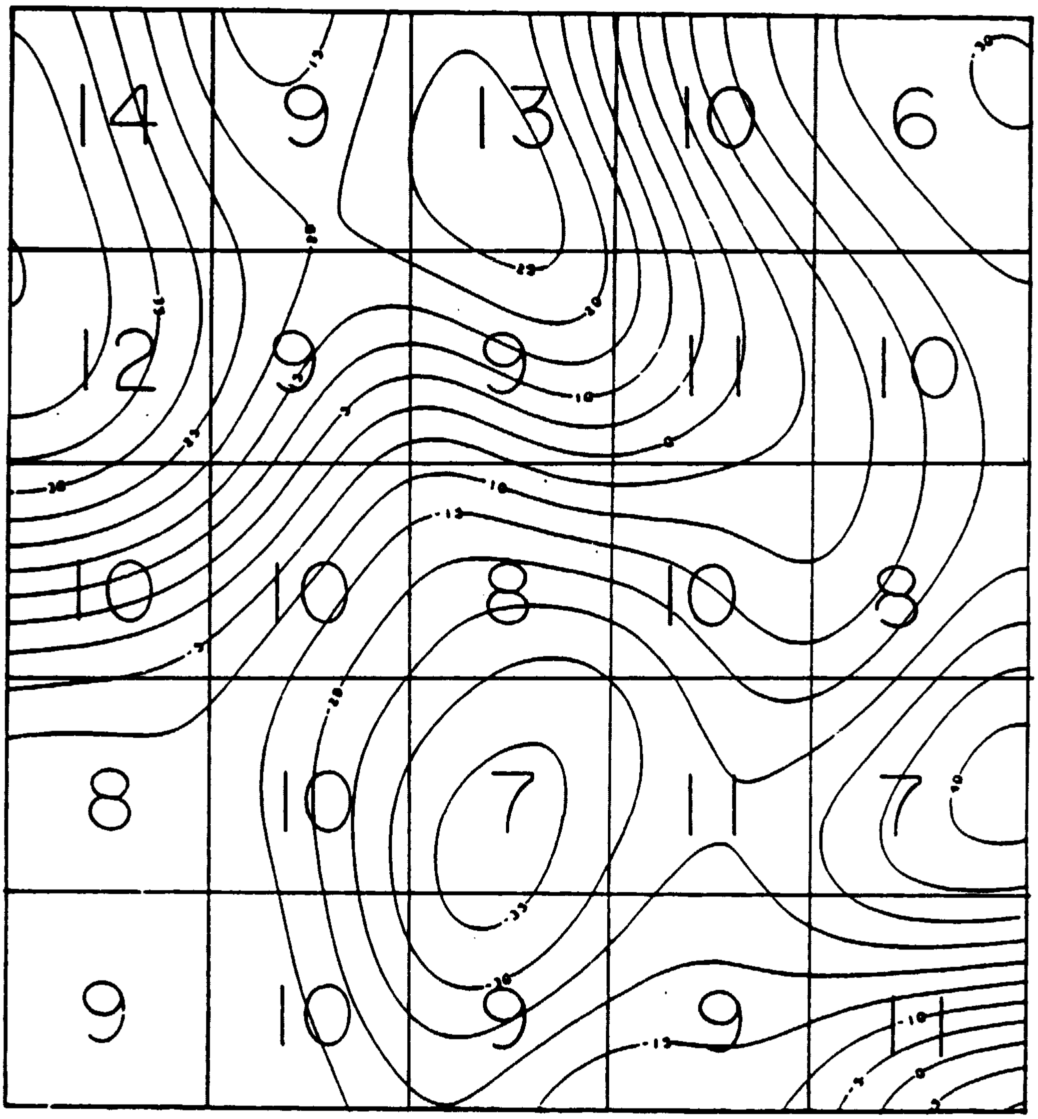

Figure 13

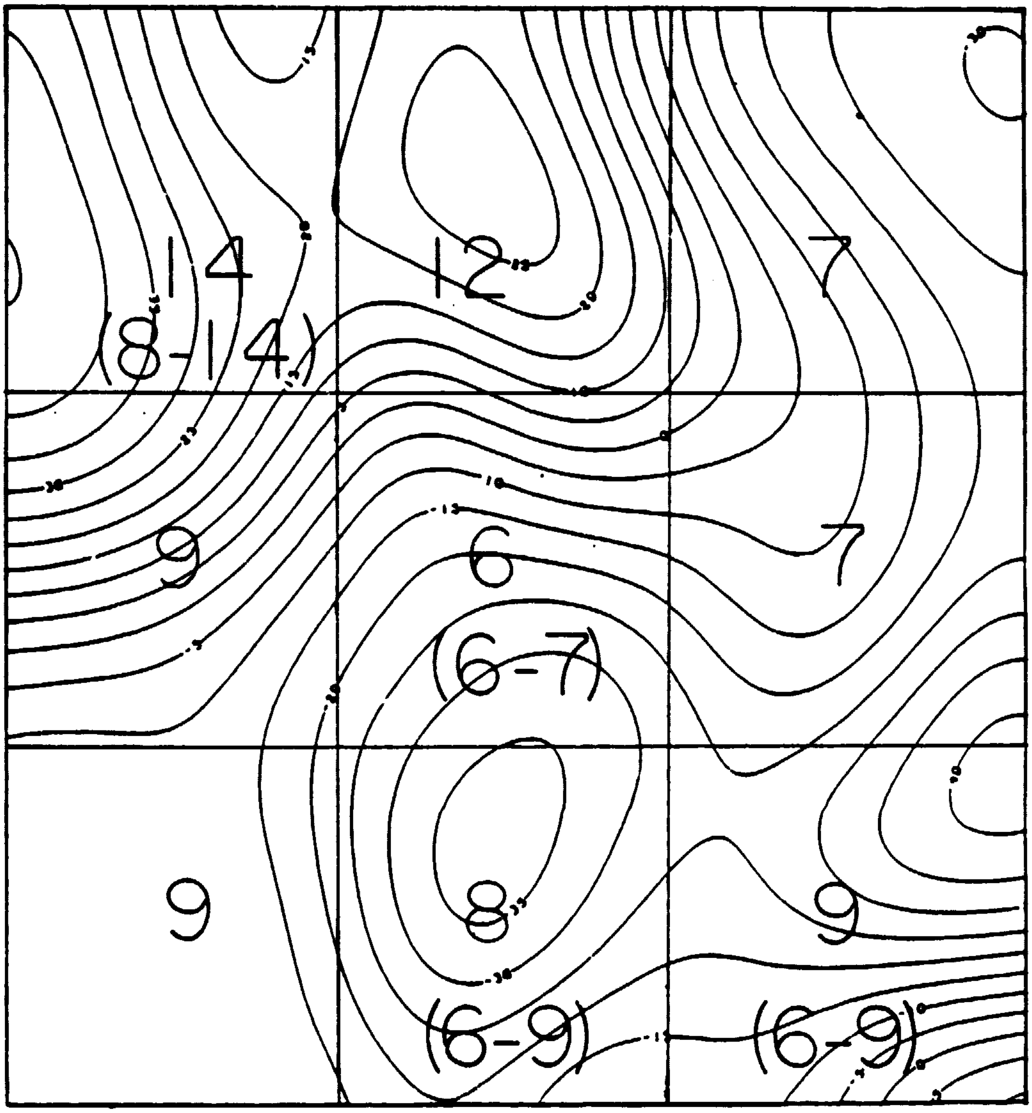

Figure 14

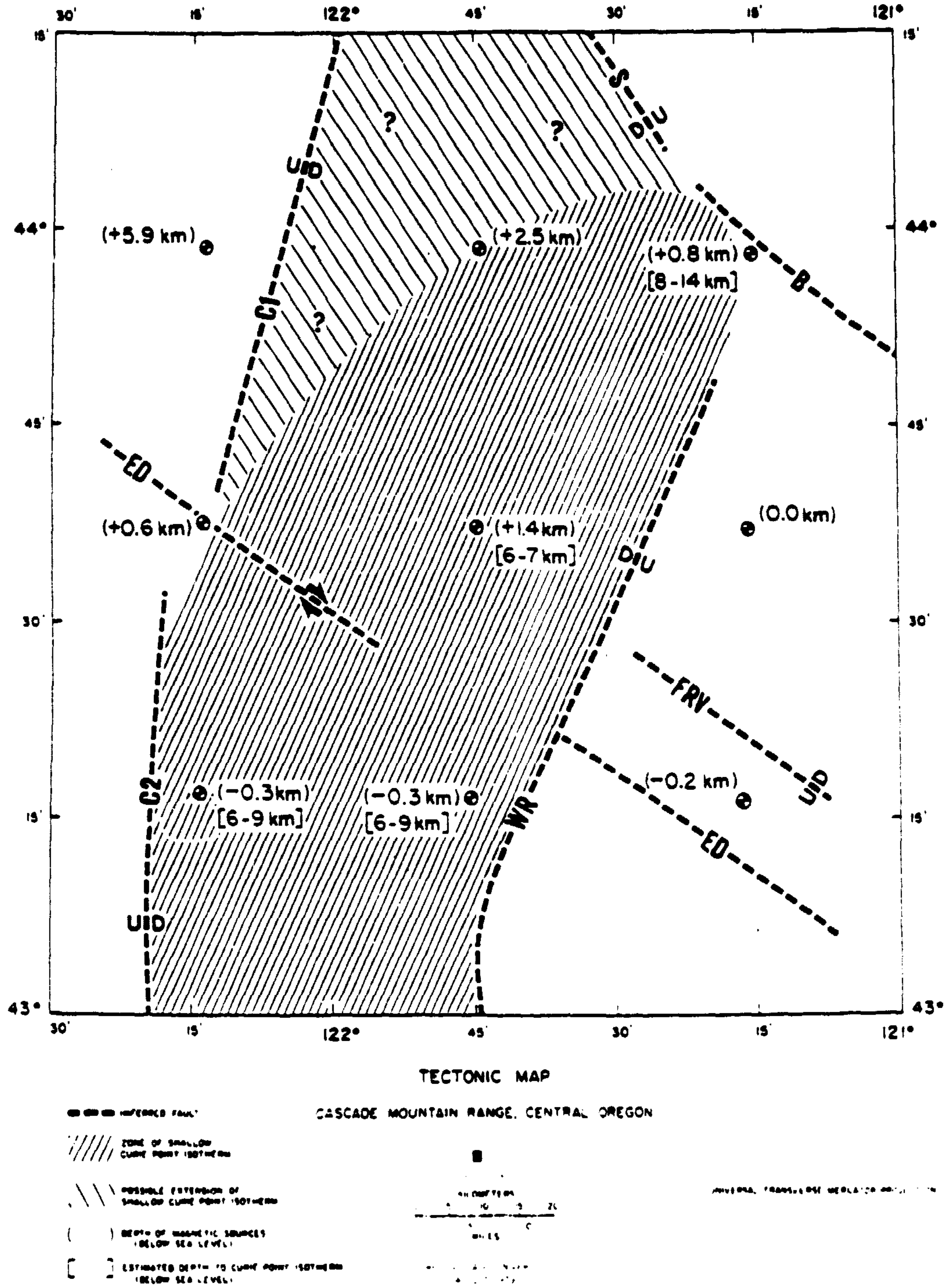

Map of the Central Oregon Cascades area showing areas of shallow Curie point isotherm and regional structural interpretation of aeromagnetic data.

Figure 15 (Connard, 1979)